Kinetically controlled synthesis of low-strain disordered micro-nano high voltage spinel cathodes with exposed {111} facets

Zhi-Qi Li[a, b], Yi-Feng Liu[a, b], Han-Xiao Liu[a, b], Yan-Fang Zhu[a, b], Jingqiang Wang[a, b], Mengke Zhang[c], Lang Qiu*[c], Xiao-Dong Guo[c], Shu-Lei Chou*[a, b] and Yao Xiao*[a, b, d]*

[a] College of Chemistry and Materials Engineering, Wenzhou University, Wenzhou, 325035, P.R. China.

[b] Wenzhou Key Laboratory of Sodium-Ion Batteries, Wenzhou University Technology Innovation Institute for Carbon Neutralization, Wenzhou, 325035, P.R. China.

[c] College of Chemical Engineering, Sichuan University, Chengdu, 610065, P.R. China.

[d] Key Laboratory of Advanced Energy Materials Chemistry (Ministry of Education), Nankai University, Tianjin 300071, P.R. China.

*Corresponding authors.

E-mail addresses: yanfangzhu@wzu.edu.cn; qiulang2023@scu.edu.cn; chou@wzu.edu.cn; xiaoyao@wzu.edu.cn.

Keywords: lithium-ion batteries, cathode materials, {111} facets, micro-nano structure, order-disorder

1.Experimental Section

1.1 Materials synthesis

The sample $LiNi_{0.5}Mn_{1.5}O_4$ was synthesized by a simple carbonate co-precipitation method and subsequent solid-state reaction. The 100 mL aqueous solution consisting of nickel sulfate hexahydrate ($NiSO_4 \cdot 6H_2O$, Sigma-Aldrich, 99.9%) and manganese sulfate monohydrate ($MnSO_4 \cdot H_2O$, Sigma-Aldrich, 99.99%) (cationic ratio of Ni/Mn=1:3) with a concentration of 2.0 mol L^{-1} were added dropwise to a tank reactor under vigorous stirring. Meanwhile, appropriate amount of 0.2 mol L^{-1} NH_4OH solution and 120 ml of 2.0 mol L^{-1} Na_2CO_3 solution were also separately pumped into the reactor. In the precipitation process, the reaction temperature was maintained at 52 °C and the pH value of the mixed solution was controlled at about 7.5, respectively. After being stirred for 4 h, the precipitate was filtrated and washed with distilled water and absolute ethanol several times to remove residual sodium and sulfuric species. After that, the precursors were dried in a vacuum oven at 80 °C for 24 h. The obtained spherical $(Ni_{0.25}Mn_{0.75})CO_3$ precursor was ground uniformly with a stoichiometric amount of Li_2CO_3 (5% excess owing to the lithium volatility during calcination). The mixtures were first calcined at 900 °C for 12 h and then cooled to 650 °C in 6 h. In addition, the furnace maintained the temperature at 650 °C for another 6 h and cooled to room temperature at a cooling rate of 1 °C min^{-1} to obtain the final product (denoted as LNMO-111). All the heat treatment processes were carried out in the air atmosphere.

1.2 Materials Characterizations

The elementary composition was determined using inductively coupled plasma mass spectrometry (ICP-MS). X-ray diffraction (XRD) pattern analysis was carried out within the range of 10° to 80° using a Bruker D8 Advance Diffractometer with a Cu Kα radiation source (λ_1 = 1.54056 Å, λ_2 = 1.54439 Å). The morphology was examined through scanning electron microscopy conducted on a field-emission microscope (SU-8020, Hitachi Limited Corporation, Japan). Further analysis involved the use of a JEOL TEM (JEM 2100F, JEOL Limited Corporation, Japan) with an acceleration voltage of 200 kV to study high-resolution transmission electron

microscopy images and energy dispersive spectroscopy mapping. X-ray photoelectron spectra were obtained from the ESCALab 250Xi (Thermo Scientific) spectrometer equipped with an Al Kα achromatic X-ray source. The final analysis involved capturing a high-angle annular dark field image using a JEOL ARM200F (JEOL, Tokyo, Japan) STEM equipped with two CEOS (CEOS, Heidelberg, Germany) probe aberration correctors at 200 kV.

1.3 Electrochemical Measurements

The cathodes were tested in CR2032 coin-type half-cells alongside lithium metal as counter electrodes. These cells were constructed in an argon-filled glove box, with water and oxygen levels carefully maintained below 0.1 ppm. Preparation of the cathode slurry involved dispersing the as-prepared cathode material, super P carbon, and polyvinylidene fluoride (PVDF, binder) in N-Methylpyrrolidone (NMP) at a weight ratio of 80:10:10. Subsequently, the mixed slurry was spread on an aluminum foil current collector and dried at 80 °C for 12 h under vacuum. The resulting electrode was then punched into a disk with an area of 0.785 cm^2, with the loading mass of active material reaching approximately 2.5 mg cm^{-2}. For the electrochemical tests, a traditional carbonate electrolyte consisting of 1M $LiPF_6$ in ethylene carbonate (EC)/dimethyl carbonate (DMC)/diethyl carbonate (DEC) (in a 1:1:1 volume ratio) was employed. To separate the cathode and anode, a porous polypropylene film (Celgard 2400) was used. The galvanostatic tests on the NEWARE Battery Test System (Shenzhen, China) involved different rates (1C = 147 mA h g^{-1}) over a voltage range of 3.5-4.9 V (*vs* Li^+/Li) and the cells were charged and discharged at the same current density.

2. Supporting figures and text

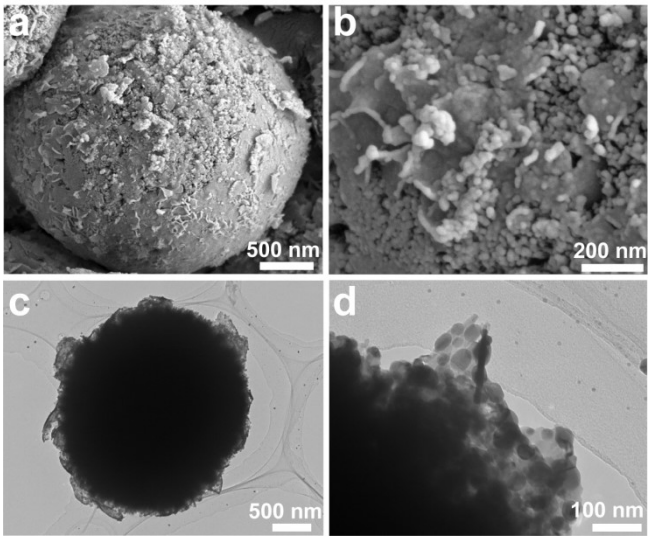

Figure S1. (a-b) SEM images of spherical $(Ni_{0.25}Mn_{0.75})CO_3$ precursor at different magnifications. (c-d) TEM images of spherical $(Ni_{0.25}Mn_{0.75})CO_3$ precursor at different magnifications.

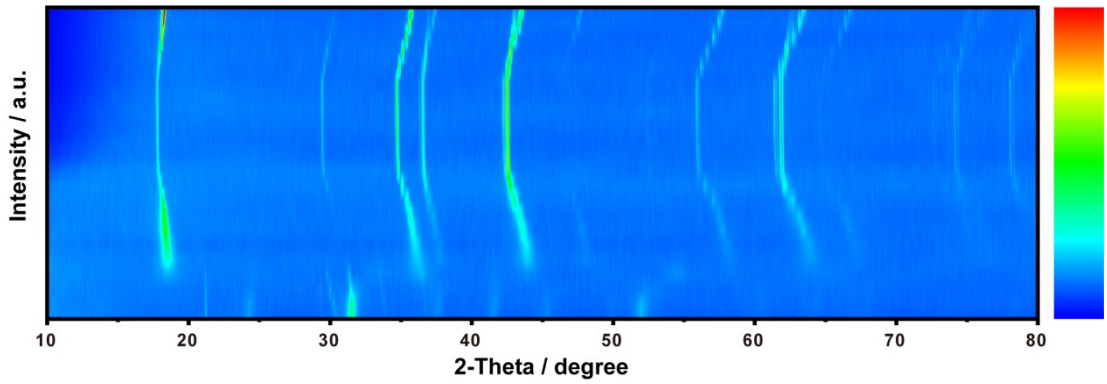

Figure S2. Contour plot of the evolution of the characteristic diffraction peaks between 10° and 80° of $Ni_{0.5}Mn_{1.5}CO_3$ precursor.

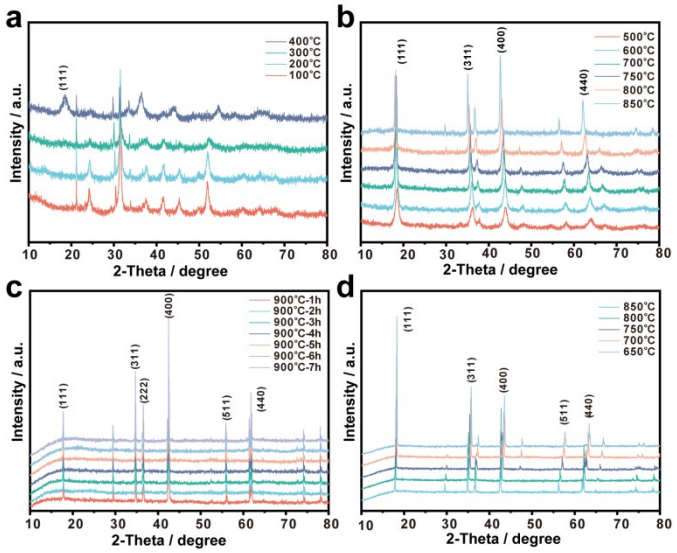

Figure S3. The structure transformation of $LiNi_{0.5}Mn_{1.5}O_4$ in different calcination temperature ranges. (a) Heating from 100 °C to 400 °C. (b) Heating from 500 °C to 850 °C. (c) maintaining at 900 °C. (d) Cooling from 850 °C to 650 °C.

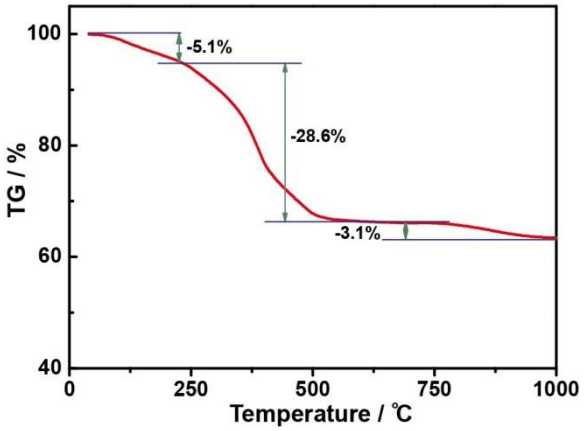

Figure S4. TG of spherical $(Ni_{0.25}Mn_{0.75})CO_3$ precursor grinded uniformly with a stoichiometric amount of Li_2CO_3.

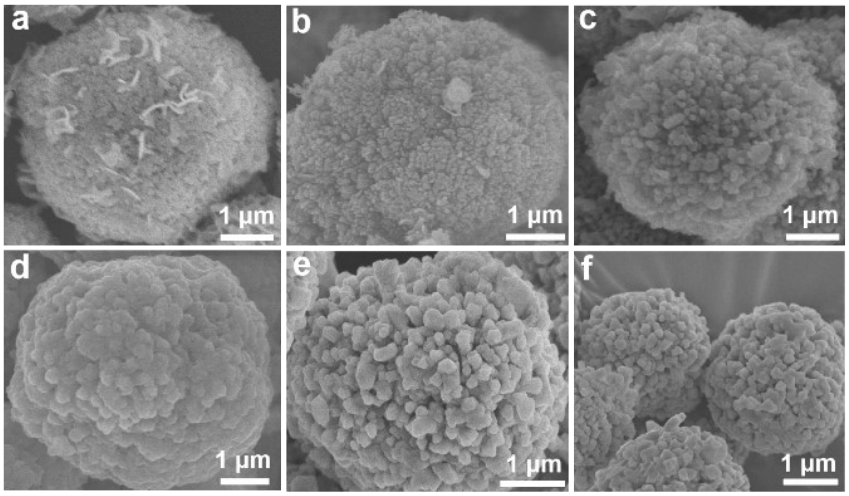

Figure S5. SEM images of precursor of LNMO-111 at different temperatures.

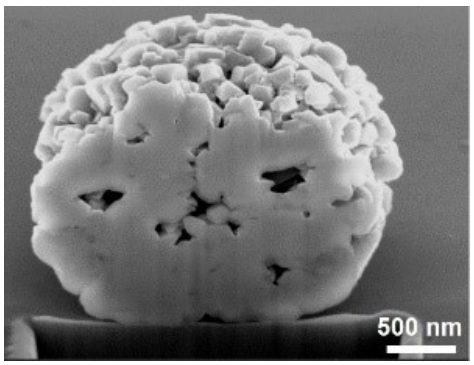

Figure S6. (a) Cross-sectional SEM image by FIB of LNMO-111 at different sites.

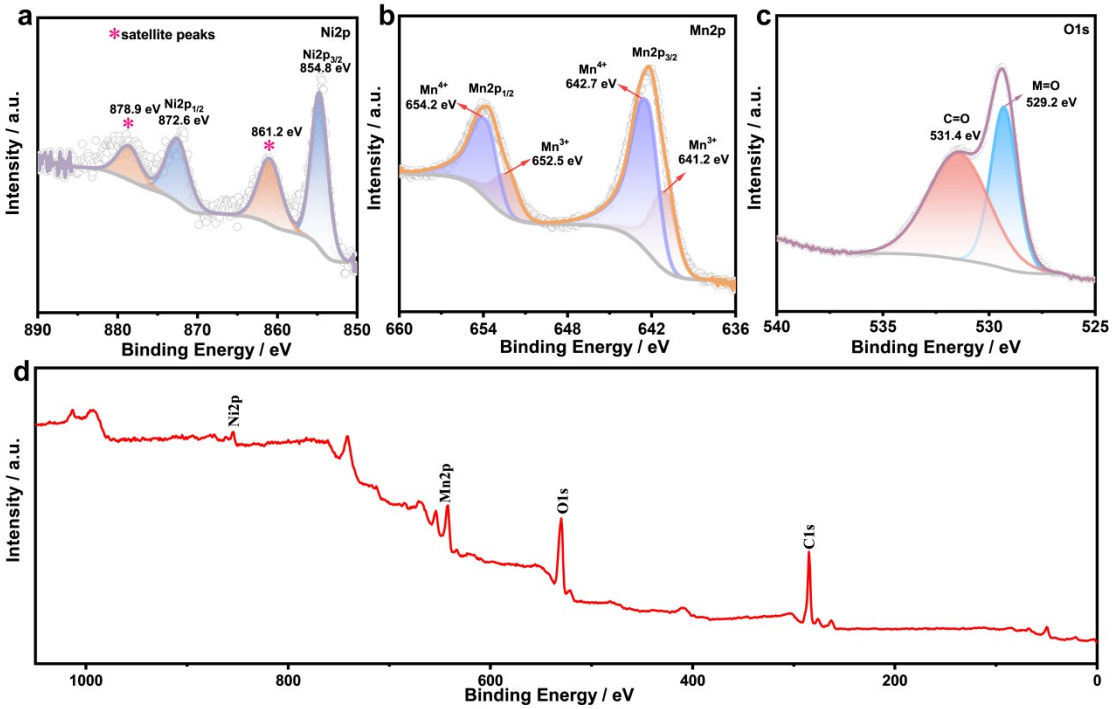

Figure S7. XPS spectra of LNMO-111 for (a) Ni 2p, (b) Mn 2p, (c) O 1s, (d) survey line, indicating nickel, manganese, and oxygen elements are in a valence state of +2, +3/+4, and −2, respectively.

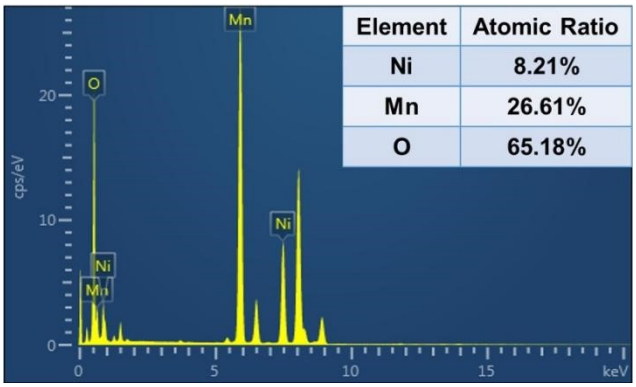

Element	Atomic Ratio
Ni	8.21%
Mn	26.61%
O	65.18%

Figure S8. EDS image of LNMO-111.

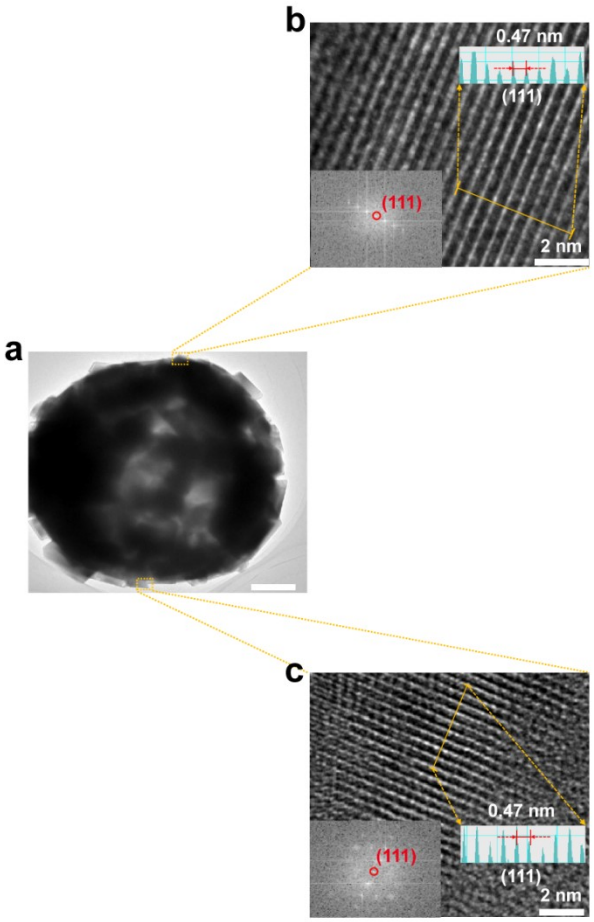

Figure S9. (a-c) TEM image and corresponding HR-TEM images of selected areas in LNMO-111.

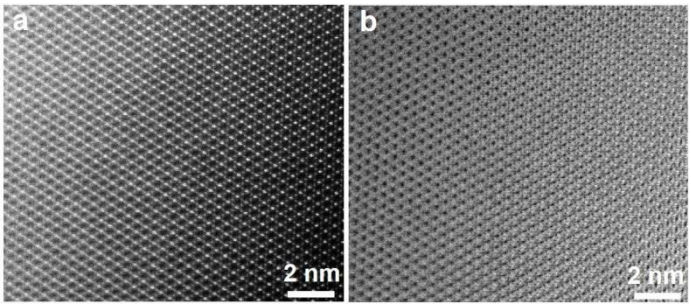

Figure S10. (a, b) HAADF- and ABF-STEM images of LNMO-111 viewed along the [110] axis.

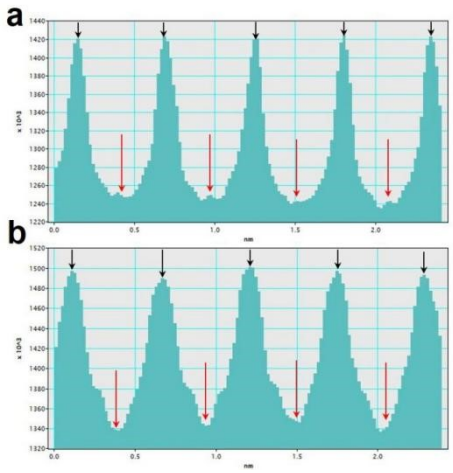

Figure S11. (a, b) Line profiles (HAADF-STEM image) of the surface and the subsurface of LNMO-111, indicating the Mn (Ni) octahedral sites (black arrows) and the empty octahedral sites (red arrows), respectively.

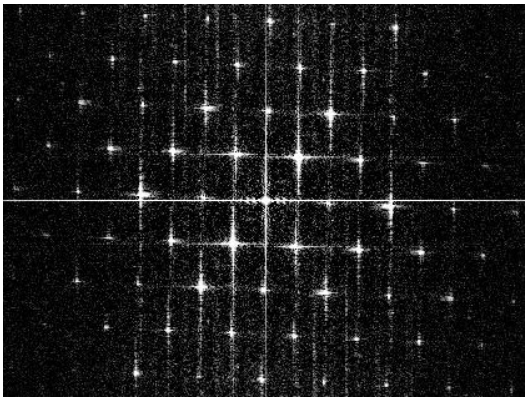

Figure S12. Typical FFT image (HAADF-STEM image) of LNMO-111 viewed along the [110] axis.

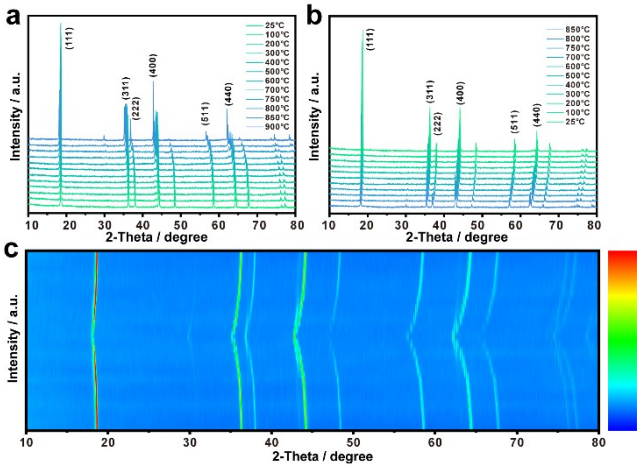

Figure S13. The structure transformation of NMO-111 in different temperature ranges. (a) Heating from 25 °C to 900 °C. (b) Cooling from 850 °C to 25 °C. (c) Contour plot of the evolution of the characteristic diffraction peaks between 10° and 80° of LNMO-111.

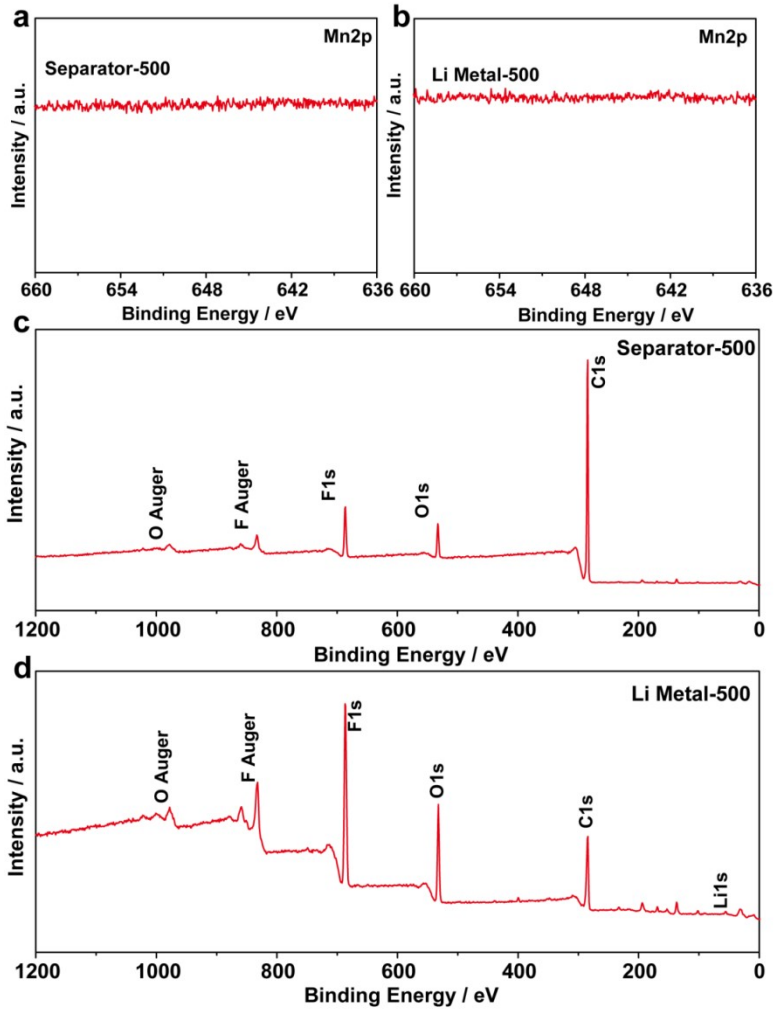

Figure S14. (a-d) XPS spectra of Mn element of the lithium metal and separator collected after 500 cycles.

Table S1. Crystallographic parameters of LNMO-111 refined by the Rietveld method.

Site	x	y	z	occ.
Li	0.1250(0)	0.1250(0)	0.1250(0)	1
Ni	0.5000(0)	0.5000(0)	0.5000(0)	0.25
Mn	0.5000(0)	0.5000(0)	0.5000(0)	Mn^{4+} (0.7238) Mn^{3+} (0.0262)
O	0.2632(0)	0.2632(0)	0.2632(0)	1
a = 8.1726(1) (Å)	V = 545.8629(6) (Å^3)	R_p = 6.22%	R_{wp} = 9.43%	

Table S2. ICP-MS results of the LNMO-111.

Theoretical chemical formula	Measured atomic ratio		
	Li	Ni	Mn
LNMO-111	0.998	0.499	1.501